Desalination and Water Treatment
www.deswater.com

doi: 10.5004/dwt.2017.21438

92 (2017) 72–79
October

Kinetic study and modelling of cephalexin removal from aqueous solution by advanced oxidation processes through artificial neural networks

Otidene R.S. da Rocha[a,*], Renato F. Dantas[b], Welenilton José do Nascimento Júnior[a], Yuji Fujiwara[a], Marta Maria Menezes Bezerra Duarte[a], Josivan Pedro da Silva[a]

[a]*Departament of Chemical Engineering, Federal University of Pernambuco, Artur de Sá s/n, Cidade Universitária, Recife, Brazil, Tel. +55 81 21267295; emails: otidene@hotmail.com (O.R.S. da Rocha), welenilton@gmail.com (W.J. do Nascimento Júnior), yujif85@gmail.com (Y. Fujiwara), mmmbduarte@gmail.com (M.M.M. Bezerra Duarte), josivan_silva@hotmail.com (J.P. da Silva)*
[b]*School of Technology, University of Campinas – UNICAMP, Paschoal Marmo 1888, 13484-332, Limeira, Brazil, email: renatofalcaod@ft.unicamp.br (R.F. Dantas)*

Received 29 March 2017; Accepted 10 September 2017

ABSTRACT

The degradation of the antibiotic cephalexin (CEX) was studied by UV direct photolysis and hydrogen peroxide combined with UVC and solar radiation. A factorial plan was used to evaluate the efficiency of the processes and the influence of variables. UVC direct photolysis had a minor contribution (12%) on CEX removal during the UV/H_2O_2 treatment. The best UV/H_2O_2 performance from the factorial plan was able to achieve a high degradation percentage for CEX and aromaticity (83.2% and 76.2%, respectively) in 60 min, while solar photolysis was not able to achieve high degradation percentage at the applied conditions. Statistical analyses pointed to the high statistical significance of the oxidant concentration for the process and the weak dependence of the other variables. The kinetic study demonstrated that the pseudo-first-order model was the more appropriate for both direct photolysis and UV/H_2O_2 treatments with rate constants of $k_{UVC} = 0.0031$ min^{-1} and $k_{UV/H_2O_2} = 0.0367$ min^{-1}. The use of artificial neural network was proven to be efficient to predict CEX removal by photolysis and photochemical treatments from aqueous solutions.

Keywords: Advanced oxidation processes; Cephalexin; Photochemical oxidation; Photolysis; Artificial neural networks

1. Introduction

The contamination of water bodies by different types of organic pollutants is an increasing concern among researchers around the world [1]. Due to the current legislations, the demand for high-quality water and effluents has increased [2]. However, some pollutants such as pharmaceuticals and personal care products have shown a high potential of persistence in different aquatic environments, being recognized in the last few years as Contaminants of Emerging Concern because of their acute toxicity and other potentially harmful effects [3–5]. Thus, many studies were focused on their toxicology [6] while others were devoted to develop alternative removal methods [7,8].

Large amounts of antibiotics have been produced in the last century [9], and their use has led to a major problem: bacterial resistance. Antibiotic residues generated by incomplete metabolism of humans and animals are released into the environment as excretion, causing and enhancing bacteria resistance [10–12]. The conventional water treatment is capable of removing only about 5% of their accumulated residues [13] since they are highly resistant to the conventional biological degradation methods [14,15].

Cephalosporins are a group of antibiotics in use since 1964, which present different antimicrobial activities. Their efficiency is associated with their low toxicity, simple utilization and effective pharmacokinetic properties [16,17]. Among this group, a semisynthetic antibiotic called cephalexin (CEX) is the largest applied cephalosporin in the world [14].

---

* Corresponding author.

CEX (Fig. 1) is a β-lactam cephalosporin named 7-(d-a-amino-a-phenylacetamide)-3-methyl-3-cephem-4-carboxylic acid monohydrate (Fig. 1) [18]. Its main properties include high solubility in water and an ample antibacterial action [19] being able to inhibit the biosynthesis of gram-positive rods and cocci and gram-negative cocci cell walls [18,20].

CEX is largely applied for human infections in respiratory and urinary systems in addition to its use in agriculture and veterinary medicine to restrain mastitis in cows [18]. Its accumulation in water bodies has been reported by several works [15,21] and it was proved that CEX could cause mutagenic and carcinogenic effects, which inspired researchers on its removal from the environment [22]. The antibiotic is also very resistant to biodegradation and conventional water treatments [23,24].

Advanced oxidation processes (AOPs) are a group of chemical oxidation techniques based on the generation of reactive radicals, which are able to degrade highly stable organic compounds, converting them into carbon dioxide, water and inorganic compounds [25–27]. The hydroxyl radical (HO•) formed by AOPs is widely applied due to its high reaction rate with the majority of organic pollutants as well as its facility of generation since it can be formed by numerous methods [27,28]. They offer a successful alternative to the degradation of persistent pollutants in wastewater and to inactivate bacteria, virus and protozoa [28,29]. Among AOPs, the UV/H_2O_2 is one of the most powerful methods to remove harmful contaminants from water. The formation of HO• is caused by radiation absorption by the H_2O_2 molecule as shown in Eq. (1) [25].

$$H_2O_2 + hv \rightarrow 2HO\cdot \quad (1)$$

UV irradiation is largely applied to treat pathogens in potable water due to its low cost [20]. UV is also able to degrade some compounds even in the absence of an oxidizing agent [28]. Some studies have reported the efficiency of H_2O_2 in the degradation of pharmaceutical organic molecules when exposed to a variety of radiations [23,30,31].

The kinetic study of complex organic molecules subjected to AOP treatments is often challenging to understand due to the lack of knowledge about the correct collection of reaction steps. The optimization of the statistical and mathematical analysis of results is the key to understand the interactions among parameters and create an effective predicting model [32]. According to Haykin [33], one of the characteristics of modelling based on artificial neural networks (ANNs) is that it does not require the physical and mathematical description of the phenomena involved in the process. ANNs have been applied to solve a great variety of tasks, which are difficult to solve, by computational programs based on simple rules such as problems associated with machine learning. They can be used as mathematical tools for non-linear problems even with multiple inputs, which make them useful to analyse compound degradation patterns in complex chemical processes [34–36]. ANN is able to generate a proper model to describe CEX degradation since it adjusts itself to face several variations on the response, which maintain the precision as high as possible.

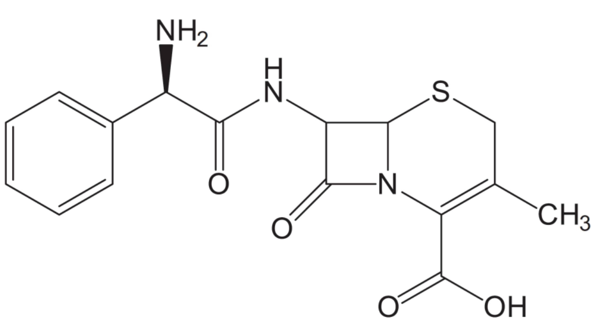

Fig. 1. Cephalexin molecular structure [16].

This study aimed to investigate the efficiency and kinetics of CEX degradation in aqueous solution by UV/H_2O_2 and UV-solar/H_2O_2 photochemical processes as well as by solar and UVC photolysis. A 2^2 factorial plan was carried out for the photochemical processes in order to study the influence of the variables in the final removal. In addition, ANN models were developed for the UVC photolysis and UVC/H_2O_2 systems to describe the degradation processes.

2. Materials and methods

CEX aqueous solutions of 150 mL at a concentration of 20 mg L^{-1} were placed in 300-mL cylindrical glass containers (9 cm of diameter and 5 cm of height). The containers were exposed either to solar radiation or to UVC light in the presence or absence of H_2O_2. The CEX used in this study was donated by *A Fórmula* pharmacy, Brazil. The concentration of the target compound was based on previous investigations found in the literature [24].

The experiments with solar radiation were conducted placing the containers on white polyethylene trays exposed to solar radiation in Recife, Brazil (8°04′03" S; 34°55′00" W) from 7:00 am to 7:00 pm. The experiments with UVC radiation were carried out in photocatalytic rectangular reactors equipped with three 30-W germicide lamps (UVC) and able of fitting 10 glass containers. The reactor luminous emittance capacity was 2,500 lux and irradiance of 53 μW cm^{-2} for 290–390 nm and 18.6 μW cm^{-2} for 254 nm.

The concentration of CEX was measured by a UV-visible fluorescence spectrometer before and after the treatment. According to Ravikumar and Gurol [37], the concentration measurement of CEX can be obtained at its greatest absorbance peak, 262 nm, and the aromaticity obtained at 254 nm. All the experiments were performed at least in duplicates to ensure reproducibility.

2.1. CEX direct photolysis

In this set of experimentation, CEX samples were exposed to UVC radiation for 720 min. Before the runs, the photocatalytic reactor was preheated for 10 min in order to stabilize the UVC light emission. Solar direct photolysis was performed at outdoor environment. Samples were withdrawn at 1, 2, 3, 4, 5, 6, 7, 8, 9, 10, 15, 20, 30, 45, 60, 120, 180, 240, 360, 480, 600 and 720 min and analysed in terms of CEX concentration and aromaticity.

2.2. Factorial planning for the photocatalytic system

For the experiments with UV/H_2O_2 and UV-solar/H_2O_2 systems, a factorial planning was used to assess the variables significance. The variables to build the 2^2 factorial planning with central point were H_2O_2 concentration (1.0, 2.0 and 3.0 mmol L^{-1}) and exposure time (30, 60 and 90 min) for both systems. H_2O_2 concentration and time used were based on previous tests. The reproducibility of the results was guaranteed by duplicate analysis of each sample and triplicate for the central point.

The software Statistic Experimental Design 6.0 was used to analyse the factorial planning data. The significance of the variables and the response surface (RS) analysis were performed using CEX removal percentage as response for both solar and UVC radiation processes.

2.3. Kinetics of CEX removal by UV/H_2O_2

To perform the kinetic study, a new experiment was carried out with the best results from the factorial plan. CEX concentration was measured at 1, 2, 3, 4, 5, 6, 7, 8, 9, 10, 15, 20, 30, 45, 60, 120, 180, 240 and 300 min of treatment.

2.4. Water quality parameters

To assess the quality of the water samples, total organic carbon (TOC), chemical oxygen demand (COD), dissolved oxygen (DO) and conductivity were analysed according to standard methodologies [38] for the samples before and after treatment.

2.5. Linear regression analysis

Zero-order, pseudo-first order and second-order linear regression models were used to verify the kinetic order of UVC photolysis and UV/H_2O_2 results. The kinetic constants (k) for both reactions were calculated from the equations of the best approximations done using regression analysis.

2.6. Kinetic modelling through ANN

The kinetic models using ANN were determined for UVC photolysis and UVC/H_2O_2 system. The ANN was built with CEX concentration and time as input variables to generate a curve of concentration over time [39,40]. For this purpose, a software was created based on C# language in Unity 3D©, commonly used to develop games and apps. The ANN was composed by input, hidden and output layers with different numbers of neurons. A group of procedures was set to make the fitting. The type of ANN used was 1:4:1 (1 input variables, 4 hidden layers and 1 output variable). The training method was based on particle swarm optimization [41,42], which a small disturbance was induced in the weights and biases to verify if the resultant network is a better adjustment according to the experimental data. Related to the computational effort, the training times last around 5 h according to the requirements of enough interactions for the adjustment. All trainings were performed on a regular desktop computer.

3. Results and discussion

3.1. CEX direct photolysis

The photolysis of CEX samples was carried out under UVC and solar radiation. The results of CEX and aromaticity removal are presented in Figs. 2 and 3, respectively.

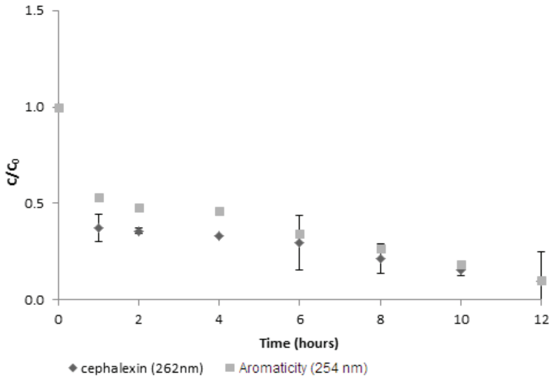

Fig. 2. Direct UVC photolysis – CEX removal vs. time (20 mg L^{-1} of CEX).

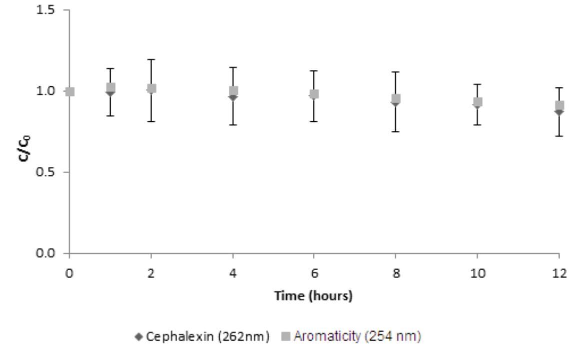

Fig. 3. Direct solar photolysis – CEX removal vs. time (20 mg L^{-1} of CEX).

According to Fig. 2, CEX was very sensitive to direct UVC photolysis since more than 50% of CEX was removed in the first hour of irradiation. Aromaticity removal had a similar profile, thus indicating that the aromatic rings from CEX structure can be transformed by UVC radiation absorption. However, when the samples were subjected to solar radiation, the CEX molecule showed to be resistant to photolysis as it can be seen in Fig. 3. Less than 10% of removal was observed after 12 h of exposure to radiation. The difference on the photolysis rate between the two used radiation sources can be explained by the higher intensity of germicide lamps in 254 nm, different from the solar radiation, which more than 99% that reaches the planet surface is UVA (400–320 nm) and UVB (320–280 nm) radiation, which are less energetic sources [28,43,44]. According to Fabbri et al. [23], radiation absorption by CEX occurs in a wavelength range near 310 nm. As expected, the breaking of intramolecular bonds in CEX was easier achieved when the radiation is higher in its peak of absorbance [28].

3.2. Factorial planning for the photocatalytic systems

Two variables were chosen to compose the factorial plan: time and H_2O_2 concentration. The results of CEX and aromaticity removal were chosen as responses and are presented in Table 1. All the analyses were carried out in duplicate and the central point in triplicate.

Table 1
Factorial plan of CEX and aromaticity removal by UV/H_2O_2 using UVC and solar radiation

H_2O_2 concentration (mmol L^{-1})	Time (min)	UVC radiation system		Solar radiation system	
		Cephalexin removal (%)	Aromaticity removal (%)	Cephalexin removal (%)	Aromaticity removal (%)
1	30	58.2	49.6	–	–
		57.5	49.6		
3	30	74.0	62.4	0.9	–
		73.9	62.3	1.1	
1	90	57.8	49.8	4.8	1.7
		59.0	51.5	2.8	
3	90	77.7	74.2	6.5	–
		76.1	72.2	5.1	
2	60	82.6	75.9	–	–
		82.5	75.9		
		84.6	76.9		

Dashes (–) indicate no significant removal observed.

The H_2O_2 performance with UVC was more efficient than the solar process as a result of the higher H_2O_2 absorption at UVC range. A significant removal was not achieved in any of the UV-solar/H_2O_2 experiments, as present in Table 1. Literature survey has shown that H_2O_2 has a very low absorption when $\lambda > 290$ nm [44], thus forming a low quantity of radicals when exposed to solar radiation. The highest CEX and aromaticity removal rates were obtained with 2 mmol L^{-1} of H_2O_2 and 60 min of treatment, which in that case corresponds to the central point of the experimental design.

The variables and their interaction effects for the UV/H_2O_2 were calculated using the data from Table 1 and the software Statistic Experimental Design 6.0. In this case, CEX removal percentage was used as response. Fig. 4 presents the study of the variables significance in a Pareto chart.

Both H_2O_2 concentration and time were statistically significant, being the H_2O_2 concentration much more significant than the tested reaction time. That behaviour was expected because the formation of HO• is directly dependent of the quantity of H_2O_2. The relationship between the two variables was not significant at the operation conditions tested in this work.

Fig. 5 presents the RS for CEX degradation, which compares the influence of the variables H_2O_2 concentration and time of exposure on CEX removal.

The RS analyses were analysed using Statistica Experimental Design software. The RS analysis corroborates with the Pareto chart since high CEX removals were achieved when higher H_2O_2 concentrations were used. That behaviour is more evident at higher reaction times. These results may suggest that higher H_2O_2 concentrations reduces photocatalytic activity since H_2O_2 works as a hydroxyl radicals scavenger [45,46], according to the following equation: $HO\bullet + H_2O_2 \rightarrow HO_2\bullet + H_2O$. In accordance with the data from Table 1, the experiments with 3 mmol L^{-1} of H_2O_2 exhibited lower degradation than experiments with 2 mmol L^{-1}, which confirms the HO• scavenging effect of H_2O_2 at the used concentration. That higher H_2O_2 disturbs the system. Therefore, the kinetic study was conducted with H_2O_2 concentration of 2 mmol L^{-1}.

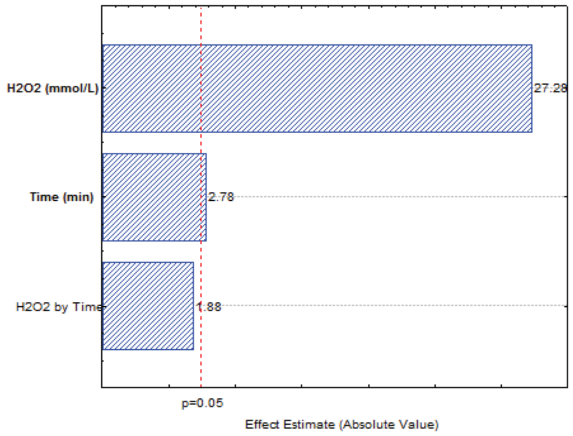

Fig. 4. Pareto chart for the UV/H_2O_2 system results from the factorial plan.

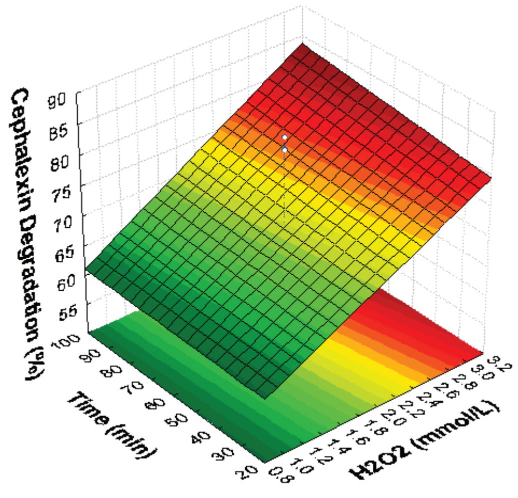

Fig. 5. Response surface analysis for CEX removal by UV/H_2O_2.

3.3. Kinetics of CEX removal by UV/H_2O_2

Fig. 6 shows the CEX and aromatics removal during an irradiation time of 300 min for the best conditions of the UV/H_2O_2 system.

After 240 min of irradiation, both CEX and aromatics were almost completely removed, achieving around 97% of degradation. It is observed by the data displayed in Fig. 6 that when HO• reacted with CEX along the time, CEX demonstrated to have higher removal rate than aromaticity. Although UVC direct photolysis favours the modification on the aromatic ring [47], HO• seems to modify preferentially other parts of CEX molecule [30].

3.4. Water quality parameters

It is well known that spectroscopy is a limited tool to measure the degradation of an organic compound during a water treatment due to the formation of by-products with similar absorbance spectrum, which can cause misinterpretation of results. However, complementary analysis can help on the assessment of the degradation. In order to have a better assessment of CEX degradation, water quality parameters were analysed after 240 min and are displayed in Table 2.

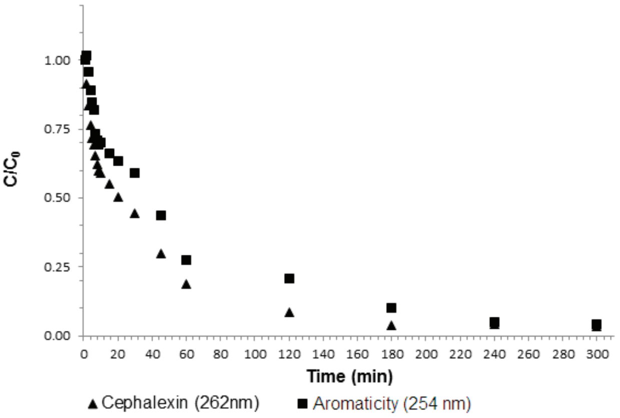

Fig. 6. CEX and aromaticity removal using 2 mmol L^{-1} of H_2O_2 during the UV/H_2O_2 system.

The TOC removal near 70% indicates that CEX degradation occurred efficiently and only organic molecules with lower molecular weight remained after treatment. According to Jung et al. [30], UV/H_2O_2-based systems are not able to achieve complete mineralization of antibiotics molecules. COD was reduced near 95% indicating that a very low remaining organic matter in the system [31].

Conductivity increase was due to the releasing of ionic species from CEX molecule. Although DO was not an important degradation parameter, the dissolved oxygen concentration in the system changes along the treatment. This result is probably influenced by the H_2O_2 photolysis and posterior formation of oxygen species.

The results obtained in the present work were compared with the literature, specifically with other degradation techniques applied for CEX removal in recent years (Table 3).

The UV/H_2O_2 system used in this work achieved similar CEX removals when compared with other advanced oxidation techniques, although higher degradations were achieved at higher reaction times. A good improvement in water quality parameters were also obtained such as the reduction in TOC and COD after treatment.

Table 2
Water quality parameter analysis for the characterization of sample before and after 4 h of treatment by UV/H_2O_2 system

Sample	TOC (mg L^{-1})	COD (mg L^{-1})	Conductivity (μS cm^{-1})	DO (mg L^{-1})
Before treatment	9.4	5.75	1.4	6.3
After treatment	2.7	0.5	30.4	11.7

Table 3
CEX degradation data by different AOP methods

CEX concentration (mg L^{-1})	Treatment method	Removal efficiency	TOC removal	COD removal	Operation time (min)	Sources
20	Ultrasound irradiation	26 % (100 W); 52 % (200 W); 35 % (400 W); and 28 % (500 W)	–	70% (150 min)	60	Guo et al. [24]
10	Photocata-lytic NiO supported on clinoptilolite nanoparticles	76%	–	74.%	300	Ajoudanian and Nezamzadeh-Ejhieh [19]
10	Photocatalytic graphene–nickel doped CdS composite	95%	–	–	180	Darwish et al. [48]
50	UV/TiO_2-coated cement beads	81%	–	80%	300	Bansal et al. [49]
20	UV/H_2O_2	97%	71%	100%	240	This work

3.5. Linear regression analysis

The data from the CEX degradation experiments with direct UVC photolysis and UV/H_2O_2 system were fitted to kinetic models of zero-order, pseudo-first-order and second-order. The results for the model fittings are presented in Table 4.

The pseudo-first-order kinetic model was the most suitable for both systems as it can be seen by the R^2 values closer to 1 (Table 4). Previous studies have found similarly pseudo-first-order model to characterize the kinetics of organic molecules degradation by AOPs with relative complexity and dependence of many reaction steps [24]. In the UV/H_2O_2 system, the H_2O_2 photolysis was rapidly achieved with the formation of high quantity of HO•, thus the kinetic constant depended only on CEX concentration. Regarding the UVC system, the CEX was the only important variable since the irradiation was enough to promote the photoreactions. These facts explain why the pseudo-first-order is an adequate model to predict the kinetics for the most part of the reaction. Second-order models would best fit the oxidation of complex mixtures of antibiotics, for example, represented by a variety of reaction pathways for different substances in the same system [23].

The estimated k_{UVC} rate constant was 0.0031 min^{-1} while k_{UV/H_2O_2} was 0.0367 min^{-1}, 12 times higher than k_{UVC}, indicating the enhancement in efficiency with the presence of H_2O_2 due to the generation of highly oxidizing species. According to the rate constant values, it is acceptable to state that the rate of reaction for the UV/H_2O_2 process had less than 12% of UVC photolysis contribution. Fabbri et al. [23] has reported 10% of photolysis contribution in the photochemical transformation of a solution of cephalosporins undergone to UVC/H_2O_2. The majority of the CEX removal was achieved by the generation of radicals, which were able to promote the cleavage of CEX molecules. Jung et al. [30] reported a great raise in rate constant when the H_2O_2 concentration is raised for a similar treatment with the antibiotic amoxicillin, justifying the results obtained in the Pareto chart (Fig. 4) and RS analysis (Fig. 5).

3.6. Kinetic modelling through ANN

ANN results from CEX degradation data for the UVC direct photolysis is presented in Fig. 7. In Fig. 7, the input layer (time of degradation) and the output layer (representing the degradation response) are exhibited. The weights (values above the lines connecting the neurons) indicate the values which multiply the output values of a neuron before the value gets to next neuron, while the bias (the arrows pointing to the neurons) indicate the added values to the neuron inputs. This model is able to predict the degradation response for the UVC photolysis process of CEX under the given conditions.

Fig. 8 shows the adjustment of the training results to the experimental data in the UVC photolysis process.

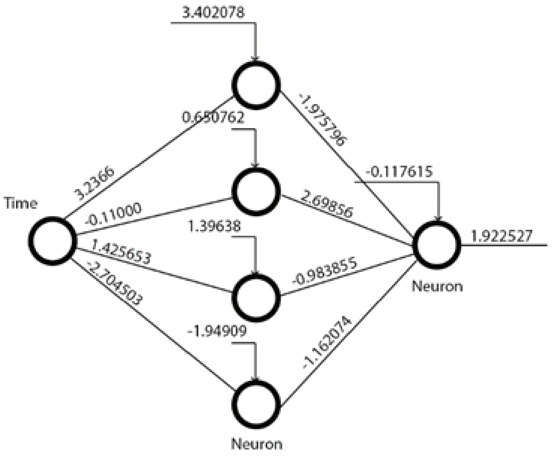

Fig. 7. ANN results of CEX UVC direct photolysis.

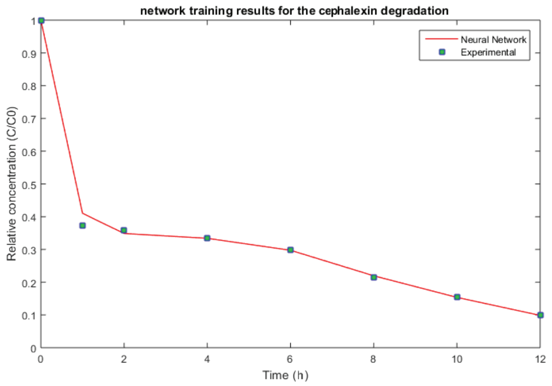

Fig. 8. Adjustment of the ANN model for UVC photolysis.

Table 4
Kinetic linear regression fittings for the treatments

AOP system	Reaction order	Equation	R^2	k (min^{-1})
UVC photolysis	Zero-order	$y = 1.8105x$	0.338	–
	Pseudo-first-order	$y = 0.1836x$	0.885	0.1836
	Second-order	$y = 0.0318x$	0.807	–
UVC/H_2O_2	Zero-order	$y = 0.2696x + 4.3919$	0.858	–
	Pseudo-first-order	$y = 0.0367x + 0.1449$	0.985	0.0367
	Second-order	$y = 0.0072x + 0.0255$	0.869	–

According to the chart, a good prediction model could be achieved by the training with a low absolute mean error estimated in 0.0192559 after 1,132,154 interactions for photolysis. It is possible to observe that ANN can detect subtle changes on experimental conditions. In Fig. 8, the experimental point at 2 h was similar when compared with the predicted result; however, the experimental point at 1 h could not fit well with the model as predicted, since in neural networks, the question of overfitting is always avoided, because the model need to generalize the set of data.

The ANN model from the CEX degradation by UV/H_2O_2 system is exhibited in Fig. 9. The result for the adjustment of the training to the experimental data in the UV/H_2O_2 process is shown in Fig. 10.

The generalization of the training was also accomplished with good performance for the UV/H_2O_2 experiment and the mean absolute error was estimated in 0.03024 after 1,437,015 interactions for the photochemical process. These results confirm that the neural network model reproduces the photodegradation of CEX and the agreement between the model predictions and the experimental data are satisfactory for both situations.

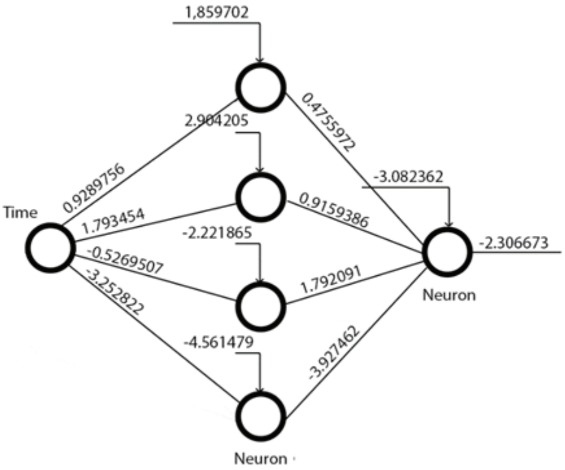

Fig. 9. ANN model of CEX degradation by UVC/H_2O_2.

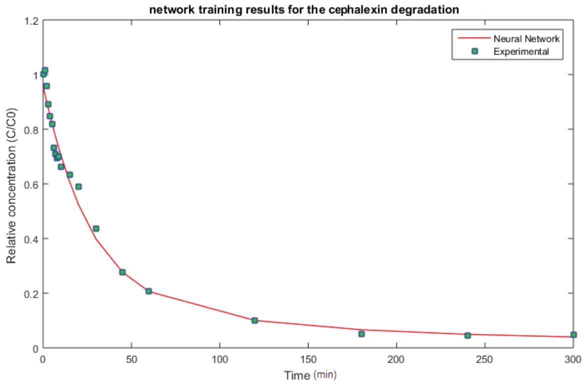

Fig. 10. Adjustment of the ANN model for UV/H_2O_2.

4. Conclusion

From the present work, it is possible to conclude that cephalexin degradation can be achieved efficiently by UV/H_2O_2 treatment. UVC direct photolysis was able to achieve considerable CEX and aromaticity removal while solar photolysis was not able to achieve significant removal. UV/H_2O_2 method was more efficient, achieving a high CEX removal rate of 97% in 240 min and improving TOC and COD. The aromatic rings seem to be faster transformed by UVC irradiation while HO• radical promotes the degradation of other parts of CEX molecule. Statistical analyses highlighted the importance of H_2O_2 concentration in the efficiency of the process. The kinetic study demonstrated that the pseudo-first-order model was the most appropriate method to describe both direct photolysis and CEX removal. The use of ANNs was proved to be an effective tool in predicting CEX removal by AOP from aqueous solutions.

Acknowledgements

The authors are thankful for the financial and resourceful support by the Brazilian National Council for Scientific Development (CNPq) and *A Fórmula* Manipulation Drugstore.

References

[1] T. Lyubimova, A. Lepikhin, Y. Parshakova, A. Tiunov A, The risk of river pollution due to washout from contaminated floodplain water bodies during periods of high magnitude floods, J. Hydrol., 534 (2016) 579–589.

[2] T. Ahmad, K. Ahmad, M. Alam, Sustainable management of water treatment sludge through 3'R' concept, J. Cleaner Prod., 124 (2016) 1–13.

[3] F. Mansour, M. Al-Hindi, W. Saad, D. Salam, Environmental risk analysis and prioritization of pharmaceuticals in a developing world context, Sci. Total Environ., 31 (2016) 557–558.

[4] M. Tankiewicz, J. Namieśnik, W. Sawicki, Analytical procedures for quality control of pharmaceuticals in terms of residual solvents content: challenges and recent developments, Trends Anal. Chem., 80 (2016) 328–344.

[5] M. Borecka, G. Siedlewicz, L.P. Haliński, K. Sikora, K. Pazdro, P. Stepnowski, A. Białk-Bielinška, Contamination of the southern Baltic Sea waters by the residues of selected pharmaceuticals: method development and field studies, Mar. Pollut. Bull., 94 (2015) 62–71.

[6] C. Gómez-Canela, T.H. Miller, N.R. Bury, R. Tauler, L.P. Barron, Targeted metabolomics of *Gammarus pulex* following controlled exposures to selected pharmaceuticals in water, Sci. Total Environ., 562 (2016) 777.

[7] F. Yu, Y. Li, S. Han, J. Ma, Adsorptive removal of antibiotics from aqueous solution using carbon materials, Chemosphere, 153 (2016) 365–385.

[8] Ö. Kerkez-Kuyumcu, Ş.S. Bayazit, M.A. Salam. Antibiotic amoxicillin removal from aqueous solution using magnetically modified graphene nanoplatelets, J. Ind. Eng. Chem., 36 (2016) 198–205.

[9] J. Ory, G. Bricheux, A. Togola, J.L. Bonnet, F. Donnadieu-Bernard, L. Nakusi, C. Forestier, O. Traore, Ciprofloxacin residue and antibiotic-resistant biofilm bacteria in hospital effluent, Environ. Pollut., 214 (2016) 635–645.

[10] W. Deng, N. Li, H. Zheng, H. Lin, Occurrence and risk assessment of antibiotics in river water in Hong Kong, Ecotox. Environ. Safety, 125 (2016) 121–127.

[11] Y. Li, Q. Li, Q. Zhou, X. Sun, L. Zhao, Y. Zhang, Occurrence and distribution of the environmental pollutant antibiotics in Gaoqiao mangrove area, China, Chemosphere, 147 (2016) 25–35.

[12] J. Wang, W. Ben, M. Yang, Y. Zhang, Z. Qiang, Dissemination of veterinary antibiotics and corresponding resistance genes from a concentrated swine feedlot along the waste treatment paths, Environ. Int., 92–93 (2016) 317–323.

[13] X. Zhang, W. Guo, H.H. Hao, H. Wen, N. Li, W. Wu, Performance evaluation of powdered activated carbon for removing 28 types of antibiotics from water, J. Environ. Manage., 172 (2016) 193–200.

[14] G. Nazari, H. Abolghasemia, M. Esmaielia, E.S. Pouya, Aqueous phase adsorption of cephalexin by walnut shell-based activated carbon: a fixed-bed column study, Appl. Surf. Sci., 375 (2016) 144–153.

[15] M. Miao, Q. Liu, L. Shu, Z. Wang, Y. Liu, Q. Kong, Removal of cephalexin from effluent by activated carbon prepared from alligator weed: kinetics, isotherms, and thermodynamic analyses, Proc. Safety Environ. Prot., 104 (2016) 481–489.

[16] W.A. Craig, D. R. Andes, Cephalosporins: Mandell, Douglas, and Benett's Principles and Practice of Infectious Diseases. 7th ed., Churchill Livingstone, London, 2009.

[17] G. Nazari, H. Abolghasemi, M. Esmaieli, Batch adsorption of cephalexin antibiotic from aqueous solution by walnut shell-based activated carbon, J. Taiwan Inst. Chem. Eng., 58 (2016) 357–365.

[18] K. Lata, R. Sharma, L. Naik, Y. S. Rajput, B. Mann, Synthesis and application of cephalexin imprinted polymer for solid phase extraction in milk, Food Chem., 184 (2015) 176–182.

[19] N. Ajoudanian, A. Nezamzadeh-Ejhieh, Enhanced photocatalytic activity of nickel oxide supported on clinoptilolite nanoparticles for the photodegradation of aqueous cephalexin, Mater. Sci. Semicond. Process., 36 (2015) 162–169.

[20] M.R. Samarghandi, T.J. Al-Musawi, A. Mohseni-Bandpi, M. Zarrabi, Adsorption of cephalexin from aqueous solution using natural zeolite and zeolite coated with manganese oxide nanoparticles, J. Mol. Liq., 211 (2015) 431–441.

[21] M.J. Ahmad, S.K. Theydan, Adsorption of cephalexin onto activated carbons from Albizia lebbeck seed pods by microwave-induced KOH and K_2CO_3 activations, Chem. Eng. J., 211–212 (2012) 200–207.

[22] Q. Kong, Y. Wang, L. Shu, M. Miao, Isotherm, kinetic, and thermodynamic equations for cefalexin removal from liquids using activated carbon synthesized from loofah sponge, Desal. Wat. Treat., 57 (2016) 7933–7942.

[23] D. Fabbri, M. Minella, V. Maurino, C. Minero, D. Vione, A model assessment of the importance of direct photolysis in the photo-fate of cephalosporins in surface waters: possible formation of toxic intermediates, Chemosphere, 134 (2015) 452–458.

[24] W. Guo, H. Wang, Y. Shi, G. Zhang, Sonochemical degradation of the antibiotic cephalexin in aqueous solution, Water SA, 2010, 36, 651.

[25] S. Giannakis, F.A. Gamarra Vives, D. Grandjean, A. Magnet, L.F. De Alencastro, C. Pulgarin, Effect of advanced oxidation processes on the micropollutants and the effluent organic matter contained in municipal wastewater previously treated by three different secondary methods, Water Res., 84 (2015) 295–306.

[26] C. Nie, N. Shao, B. Wang, D. Yuan, X. Sui, H. Wu, Fully solar-driven thermo- and electrochemistry for advanced oxidation processes (STEP-AOPs) of 2-nitrophenol wastewater, Chemosphere, 154 (2016) 604–612.

[27] M. Cheng, G. Zeng, D. Huang, C. Lai, P. Xu, C. Zhang, Y. Liu, Hydroxyl radicals based advanced oxidation processes (AOPs) for remediation of soils contaminated with organic compounds: a review, Chem. Eng. J., 284 (2016) 582–598.

[28] Y. Xu, Z. Lin, H. Zhang, Mineralization of sucralose by UV-based advanced oxidation processes: UV/PDS vs. UV/H_2O_2, Chem. Eng. J., 285 (2016) 392–401.

[29] Y. Zhang, Y. Zhuang, J. Geng, H. Ren, K. Xu, L. Ding, Reduction of antibiotic resistance genes in municipal wastewater effluent by advanced oxidation processes, Sci. Total Environ., 550 (2016) 184–191.

[30] Y.J. Jung, W.G. Kim, Y. Yoon, J. Kang, Y.M. Hong, H.W. Kim, Removal of amoxicillin by UV and UV/H_2O_2 processes, Sci. Total Environ., 420 (2012) 160–167.

[31] W. Guo, Y. Shi, H. Wan, H. Yang, G. Zhang, Intensification of sonochemical degradation of antibiotics levofloxacin using carbon tetrachloride, Ultrason. Sonochem., 17 (2010) 680–684.

[32] S.N. Sanusi, M.E. Halmi, S.S. Abdullaha, H.A. Hassana, F. M. Hamzahb, M. Idris, Comparative process optimization of pilot-scale total petroleum hydrocarbon (TPH) degradation by *Paspalum scrobiculatum* L. Hack using response surface methodology (RSM) and artificial neural networks (ANNs), Ecol. Eng., 97 (2016) 524–534.

[33] S. Haykin, Redes Neurais: Princípios e Práticas, 5th ed., Artmed, São Paulo, 2001, pp. 28–45.

[34] R. Willumeit, F. Freyerabend, N. Huber, Magnesium degradation as determined by artificial neural networks, Acta Biomaterialia, 9 (2013) 8722–8729.

[35] L. Das, U. Maity, J.K. Basu, The photocatalytic degradation of carbamazepine and prediction by artificial neural networks, Proc. Safety Environ. Prot., 92 (2014) 888–895.

[36] D. Bingöl, M. Hercan, S. Elevli, E. Kiliç, Comparison of the results of response surface methodology and artificial neural network for the biosorption of lead using black cumin, Biores. Technol, 112 (2012) 111–115.

[37] J.X. Ravikumar, M.D. Gurol, Chemical oxidation of chlorinated organics by hydrogen peroxide in the presence of sand, Environ. Sci. Technol., 28 (1994) 393.

[38] APHA, AWWA, WEF, Standard Methods for the Examination of Water and Wastewater, American Public Health Association, American Water Works Association and Water Environment Federation, New York, 2005.

[39] S. Göb, E. Oliveros, S.H. Bossmann, A.M. Braun, R. Guardani, C. A. O. Nascimento, Modeling the kinetics of a photochemical water treatment process by means of artificial neural networks, Chem. Eng. Proc., 38 (1999) 373–382.

[40] J.A. Giroto, R. Guardani, A.C.S.C. Teixeira, C.A.O. Nascimento, Study on the photo-Fenton degradation of polyvinyl alcohol in aqueous solution, Chem. Eng. Proc., 45 (2006) 523–532.

[41] J. Kennedy, R. Eberhart, Particle Swarm Optimization, IEEE International Conference, 1995.

[42] S. Haikin, Neural Networks: A Comprehensive Foundation, 2nd. ed., Prentice Hall, Upper Saddle River, 1999.

[43] C. Lin, H. Lin, L. Hsu, Degradation of ofloxacin using UV/H_2O_2 process in a large photoreactor, Sep. Purif. Technol., 168 (2016) 57–61.

[44] D. Rubio, E. Nebot, J.F. Casanueva, C. Pulgarin, Comparative effect of simulated solar light, UV, UV/H_2O_2 and photo-Fenton treatment (UV–Vis/H_2O_2/$Fe^{2+,3+}$) in the *Escherichia coli* inactivation in artificial seawater, Water Res., 47 (2013) 6367–6379.

[45] F.V. Araújo, L. Yokoyama, L.A. Teixeira, Quím. Nova, 9 (2006) 11.

[46] E.R.L. Tiburtius, P.P. Zamora, E.S. Leal, Quím. Nova, 27, (2004) 441.

[47] W. Zhang, C.R. Wilson, N.D. Danielson, Indirect fluorescent determination of selected nitro-aromatic and pharmaceutical compounds via UV-photolysis of 2-phenylbenzimidazole-5-sulfonate, Talanta, 74 (2008) 1400–1407.

[48] M. Darwish, A. Mohammadi, N. Assi, Integration of nickel doping with loading on graphene for enhanced adsorptive and catalytic properties of CdS nanoparticles towards visible light degradation of some antibiotics, J. Hazard. Mater., 320 (2016) 304–314.

[49] P. Bansal, A. Verma, K. Aggarwal, A. Singh, S. Gupta, Investigations on the degradation of an antibiotic cephalexin using suspended and supported TiO_2: mineralization and durability studies, Can. J. Chem. Eng., 94 (2016) 1269–1276.